Mechanical Controls on Solute Transport and Methane Bubble Growth Characteristics within Muddy Aquatic Sediment

Xiongjie Zhou

Supervisor: Dr. Regina Katsman

Department of Marine Geosciences

University of Haifa

1. Introduction

Observations

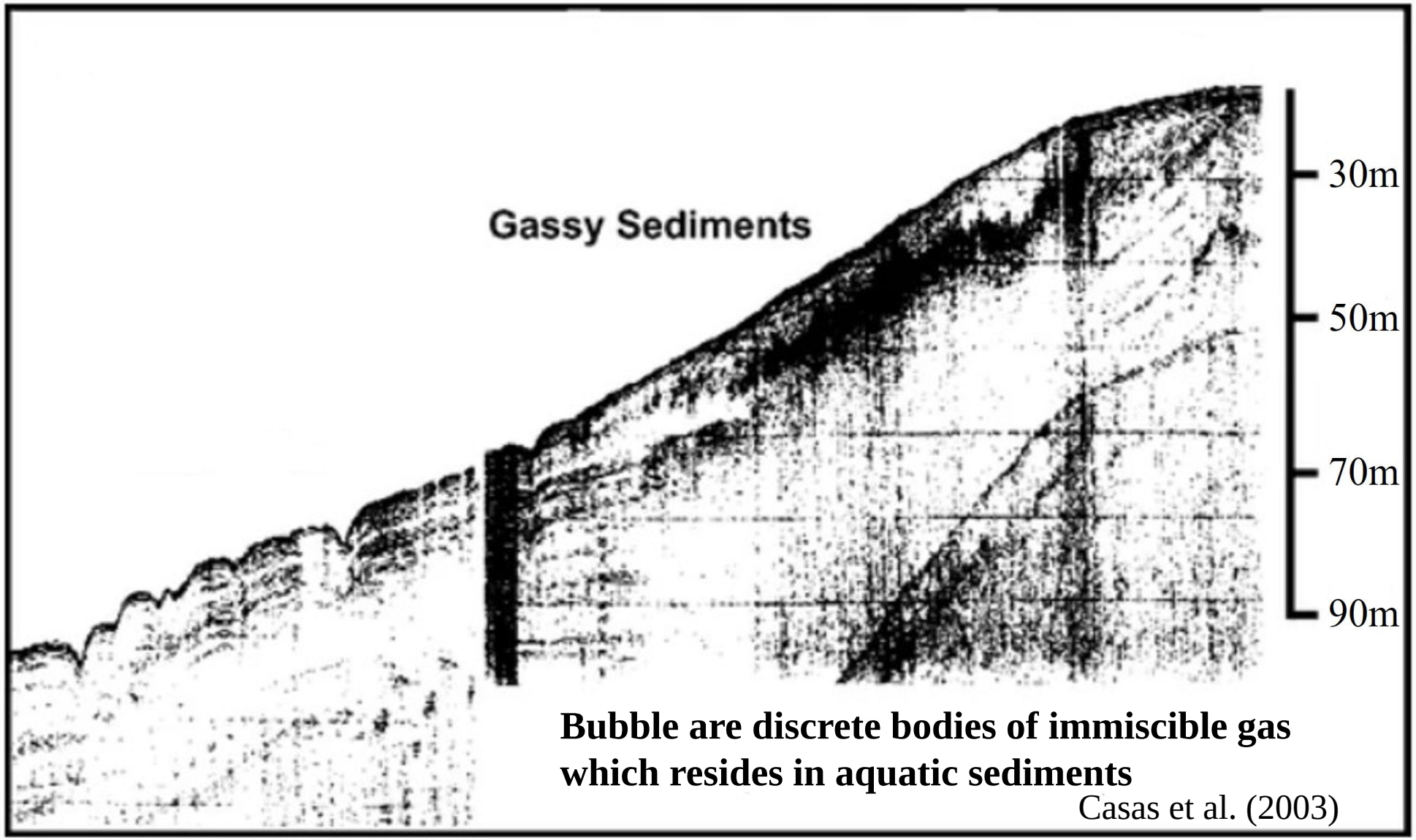

Bubble are discrete bodies of immiscible gas which resides in aquatic sediments

Casas et al. (2003)

1. Introduction

Bubbles structures in aquatic sediments

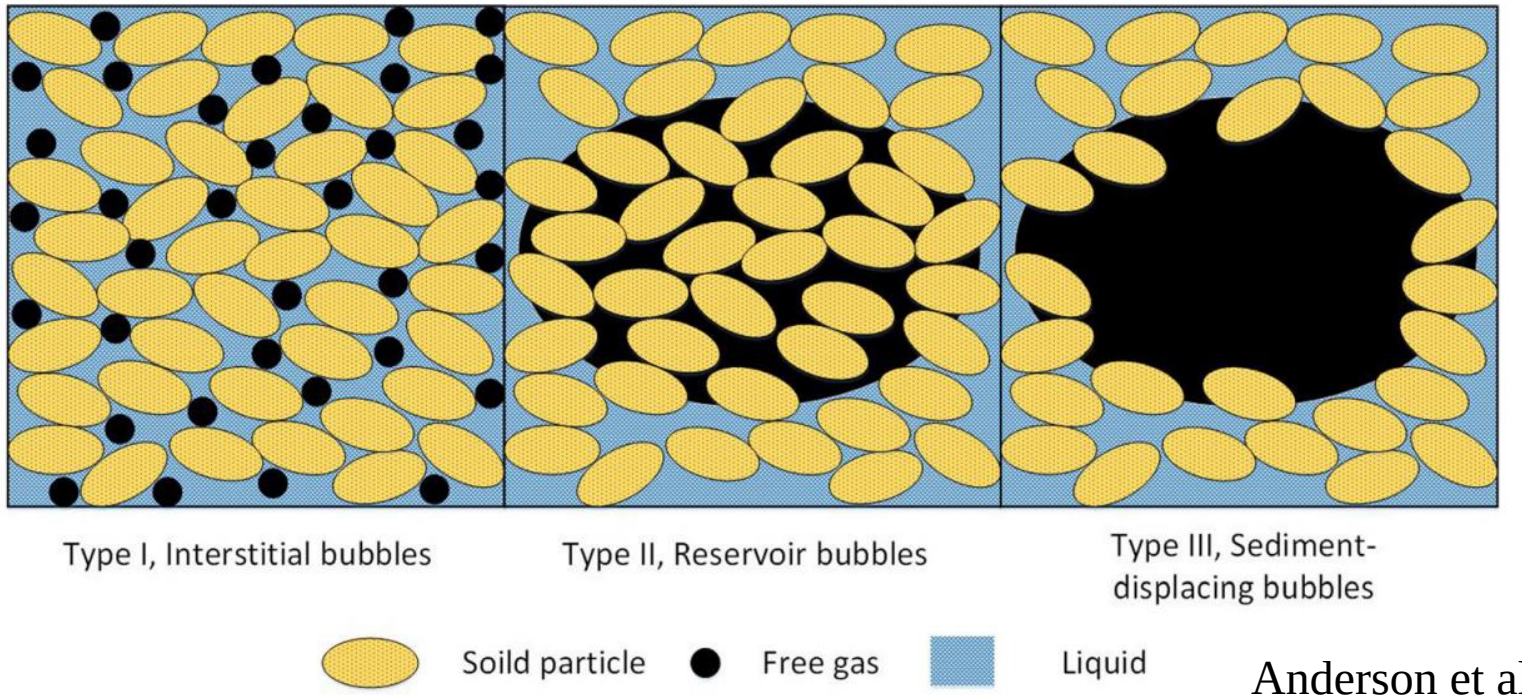

Anderson et al. (1998)

- Type I: A framework of deposited particles filled with two phases (solid-liquid) ;
- Type II: Bubbles filling the void spaces between the bulk particles only displace the pore water, while the grains remain in place (coarse-grained sediments such as sand and gravel);
- Type III: Bubbles displace pore water and solid particles (dominant form in muddy sediments, Best et al., 2006)

1. Introduction

Bubble shape and growth mechanism

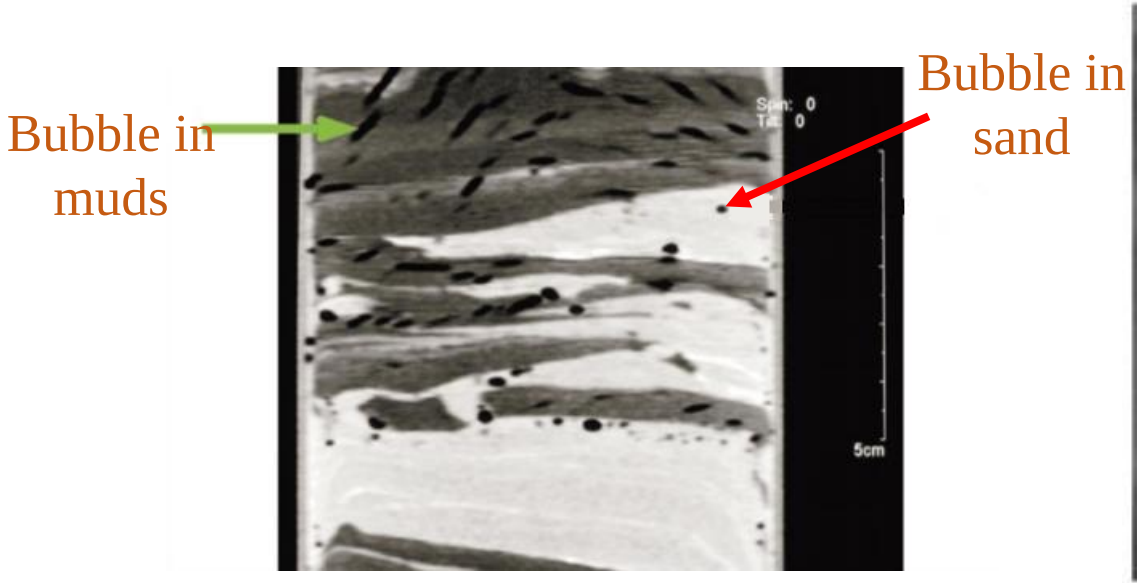

Boudreau et al. (2005)

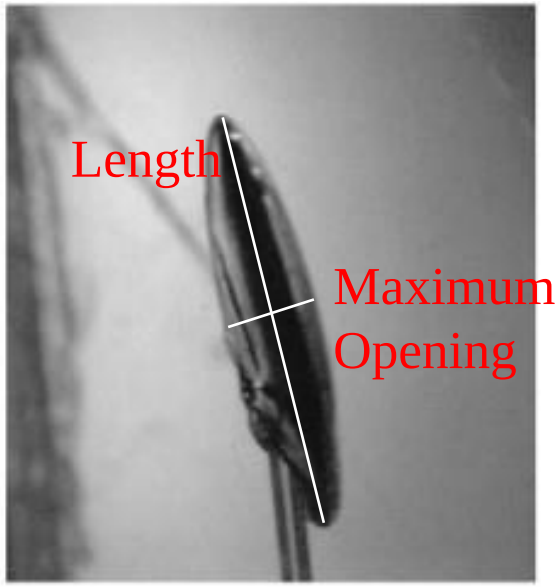

Johnson et al. (2002)

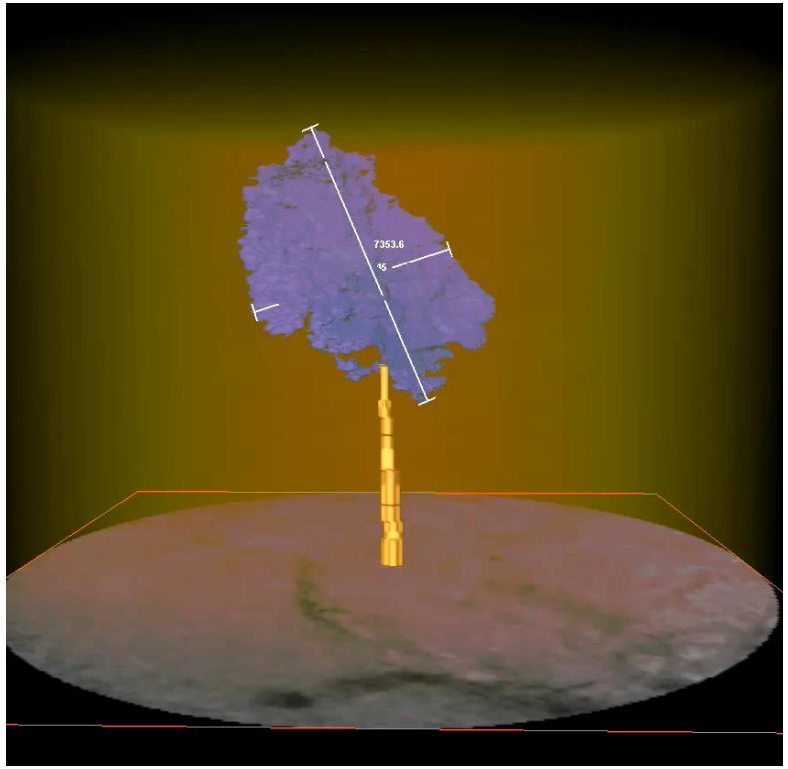

Boudreau et al. (2005)

Bubbles grow in muddy sediments, initially filling adjacent pore spaces and then beginning to deform the surrounding sediment skeleton (Van Kessel and van Kesteren, 2002; Johnson et al., 2002)

1. Introduction

Two processes managing bubble growth in muddy sediments:

- CH_4 solute supply to the growing bubble
- Linear elastic fracture mechanics (LEFM) that manages the mechanical response of ambient muddy sediments

1. Introduction

Linear Elastic Fracture Mechanics (LEFM)

Fracture Toughness K_{IC}

Fracture Toughness: a quantitative way of expressing a material's resistance to fracture associated with breaking the cohesion between the grains.

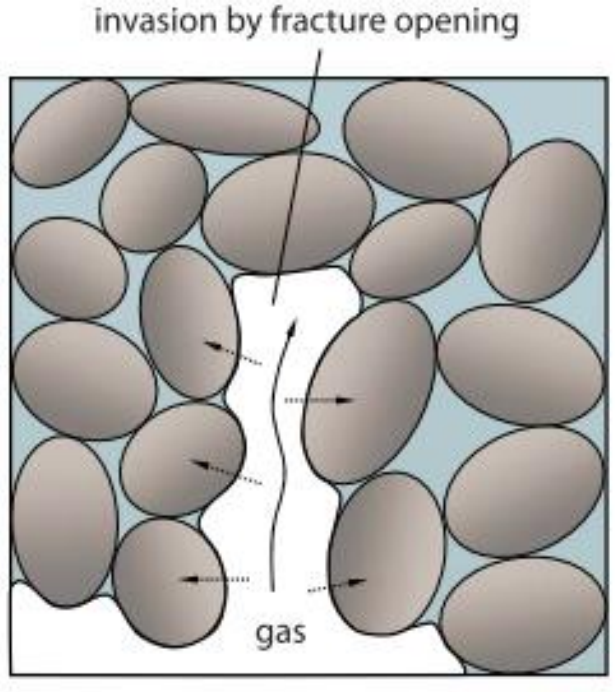

Jain and Juanes (2009)

1. Introduction

Linear Elastic Fracture Mechanics (LEFM)

Young’s modulus

Young's modulus: A mechanical property that measures the tensile or compressive stiffness of a solid material.

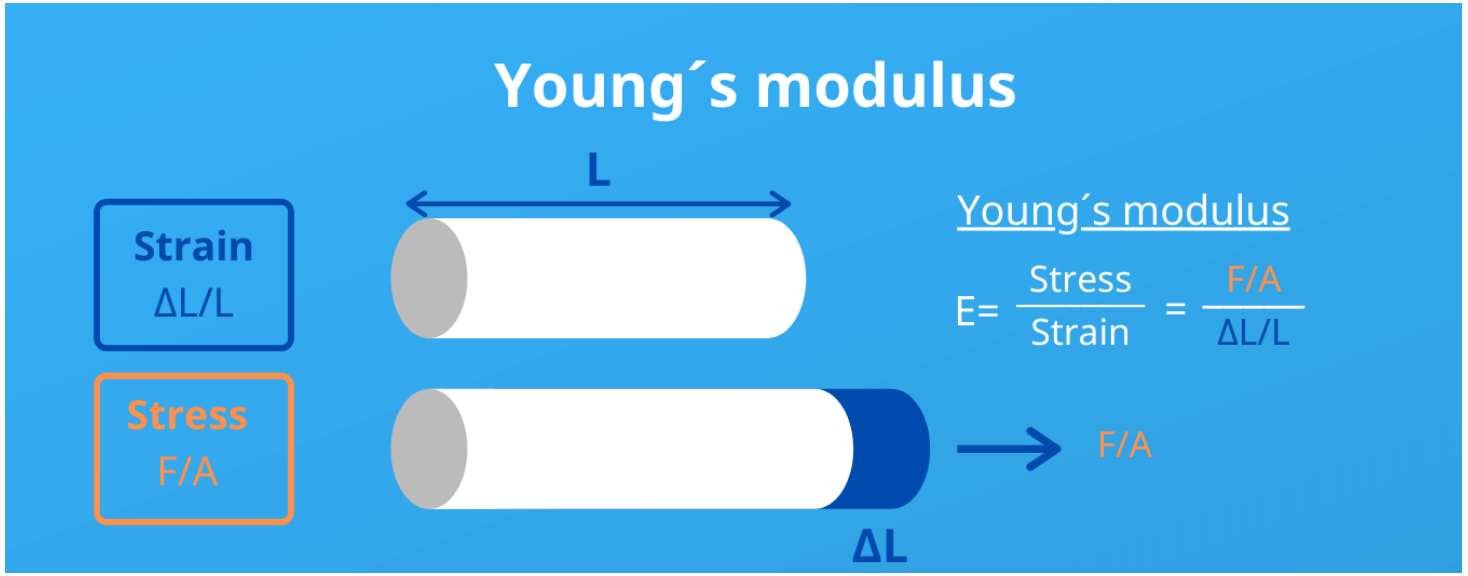

1. Introduction

Bubble growth mechanism

Measuring the internal pressure of bubbles as they grow in the muddy sediment, Johnson et al. (2002) revealed:

- **the internal pressure exhibits a saw-tooth pattern;**
- **the pattern is expected if the tested sediment responds to an increment of pressure in an elastic manner, but eventually fails by fracturing;**
- **a saw-tooth pattern cannot be associated with plastic or fluid responses**

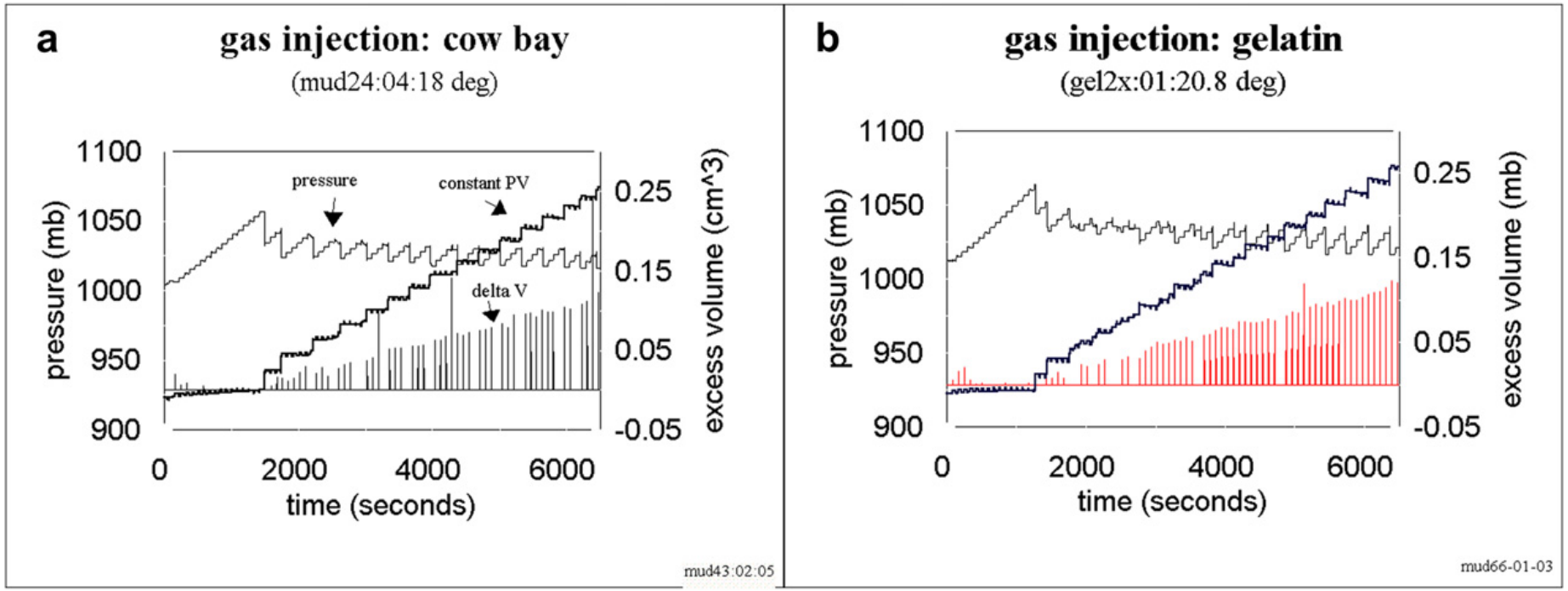

1. Introduction

Elastic Fracturing-Solute Transport System

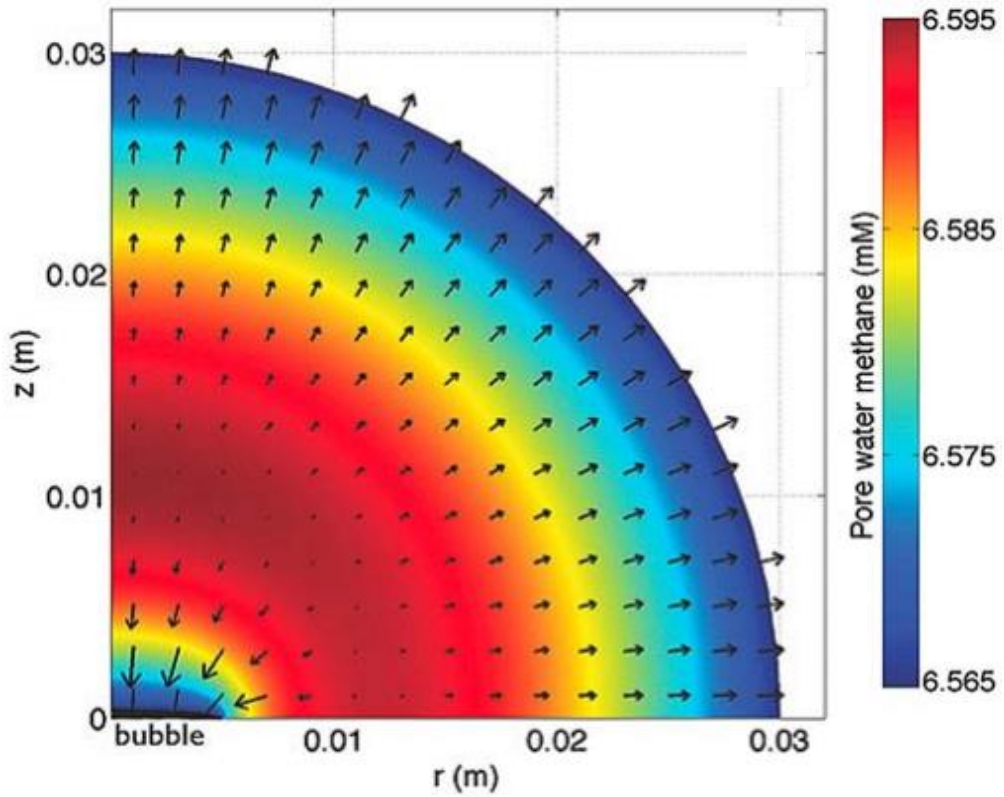

Bubble uptake the solute during elastic expansion

Algar and Boudreau (2010)

One quarter of a slice through the sediment

Solute transport and elastic fracturing are the two main coupled processes that drive the bubble growth.

2. Knowledge Gaps

(1) The effects of the sediment mechanical properties controlling the bubble growth for solute transport are less important (e.g. Algar and Boudreau, 2009), which requires further investigation.

(2) The effects of the coupling have not been investigated and need to be explored in depth.

3. Research Objectives

- To understand solute exchange process of the growing premature bubble with ambient muddy sediment under different sediment mechanical properties (fracture toughness and Young's modulus) and to identify specific roles in the bubble growth dynamics.
- To study various bubble growth characteristics (e.g., inner bubble pressure, solute fluxes, bubble growth rate, bubble shape and size) as a function of sediment mechanical properties.
- To get insights into various aspects and implications of the investigated coupling between the bubble solute transport and muddy sediment mechanical response.

4. Materials and Methods

Model: Geometry

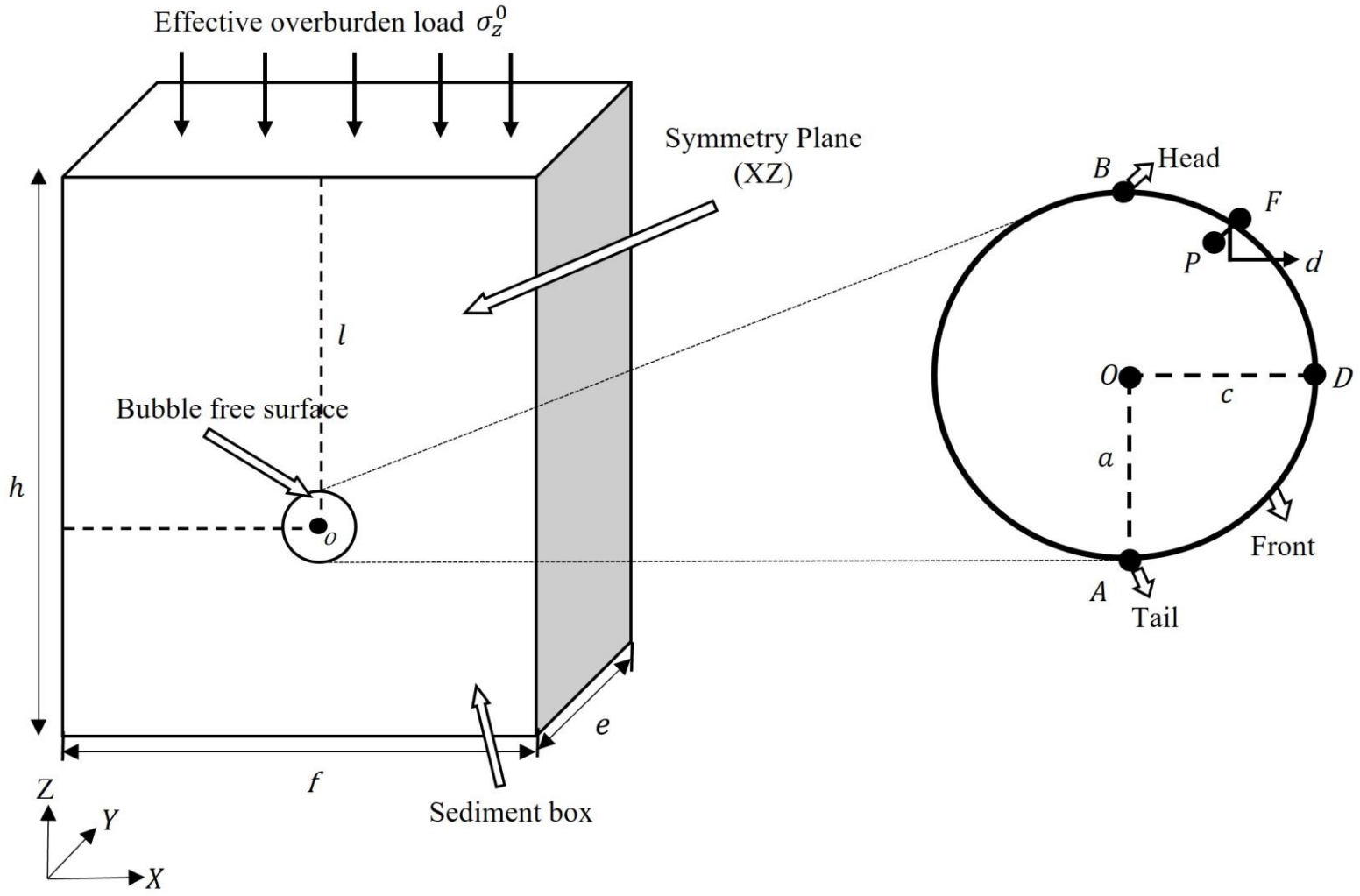

A bubble is modeled as a small penny-shaped crack with one surface placed on the symmetry plane (XZ)

The advantage of this model is in the two-way coupling of the continuous solute transport component, with a Linear Elastic Fracture Mechanics component

4. Materials and Methods

Model: Bubble growth configuration

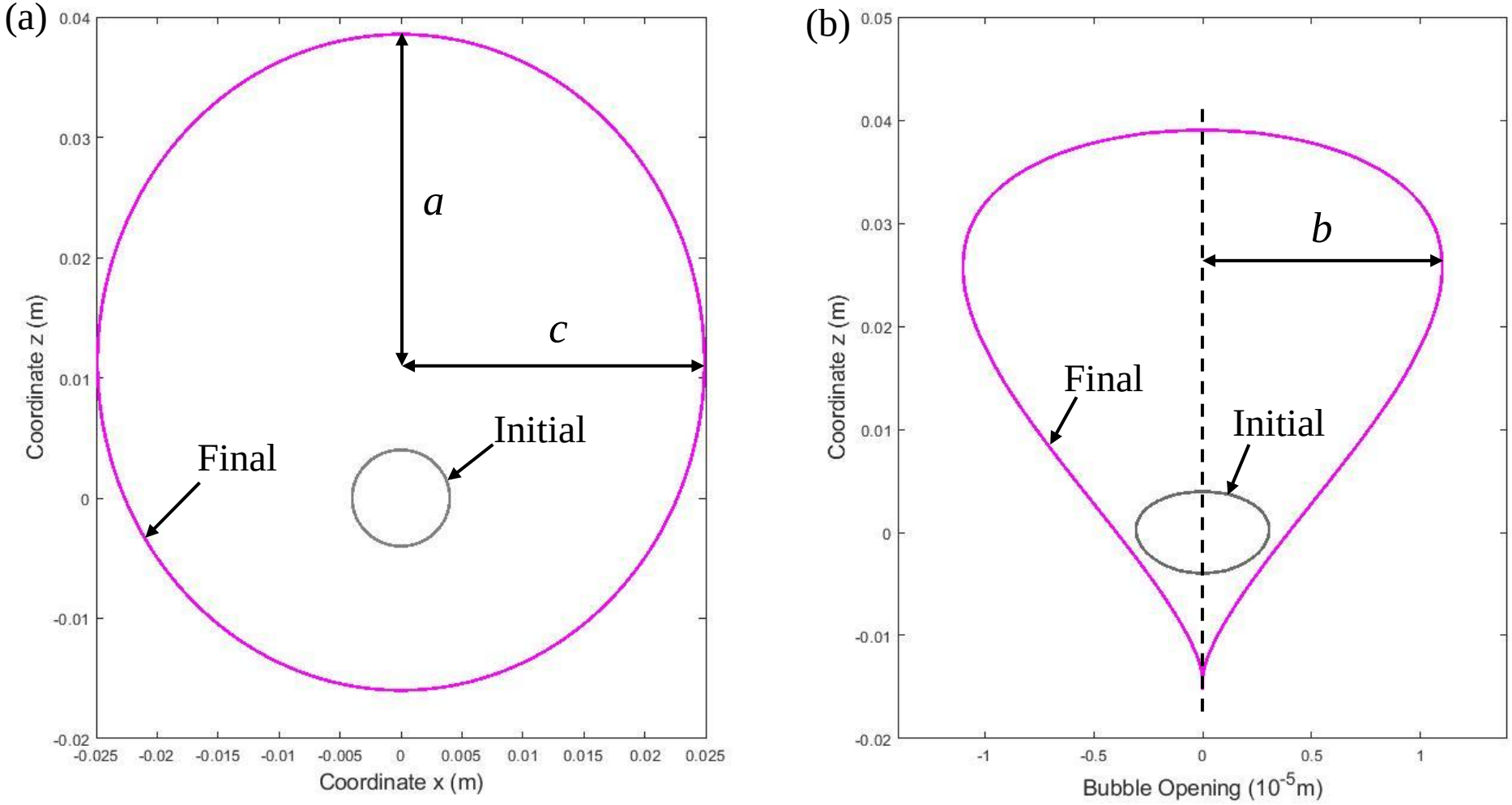

Front view (panel a) and opening over the main cross-section (panel b) from initial penny-shaped bubble (in gray) to final elliptic mature bubble (in magenta).

4. Materials and Methods

Main equations solved in the model

Solute conservation equation in porous sediment box

$$\frac{\partial C_{CH_4(aq)}}{\partial t} + \nabla \cdot \left[-D \nabla C_{CH_4(aq)}\right] = S_{CH_4}$$

Conservation of gaseous CH_4 inside the bubble

$$\frac{\partial \left(C_{CH_4(g)} V_b\right)}{\partial t} = \int_{\alpha} \vec{n} \cdot \left(-D \emptyset \nabla C_{CH_4(aq)}\right) d\alpha$$

Concentration of dissolved CH_4 at the bubble surface (Henry's Law)

$$C_{CH_4(aq)}(\alpha, t) = C_{CH_4(g)} \cdot k_H$$

Stress intensity factor (SIF) at the bubble front

$$K_I = \frac{E}{4(1-v^2)} \sqrt{\frac{\pi}{2r}} 2w_n^P$$

4. Materials and Methods

Fracture Toughness and Young's modulus setting in the model

Parameters/variables	value
Fracture Toughness	$K_{Ic} = 30,\ 40,$ 60 ** $70\ Pa \cdot m^{1/2}$(Johnson et al., 2002, 2012)
Young's modulus	$E = 4 \times 10^5$ 5.5×10^5 **, $7 \times 10^5 Pa$ (Anderson and Hampton, 1980; Algar and Boudreau, 2010; Barry et al., 2012)

The proportionality could be derived from LEFM, suggesting K_{Ic}/E~10^{-4} $m^{1/2}$ order of magnitude is indicative for the basic values of Fracture Toughness and Young's modulus

The absolute values of K_{Ic} and E are assigned in this study to vary slightly, to investigate the effects of each parameter.

5. Results

Evolution of maximal Stress Intensity Factor (SIF) K_{Imax} over the bubble front

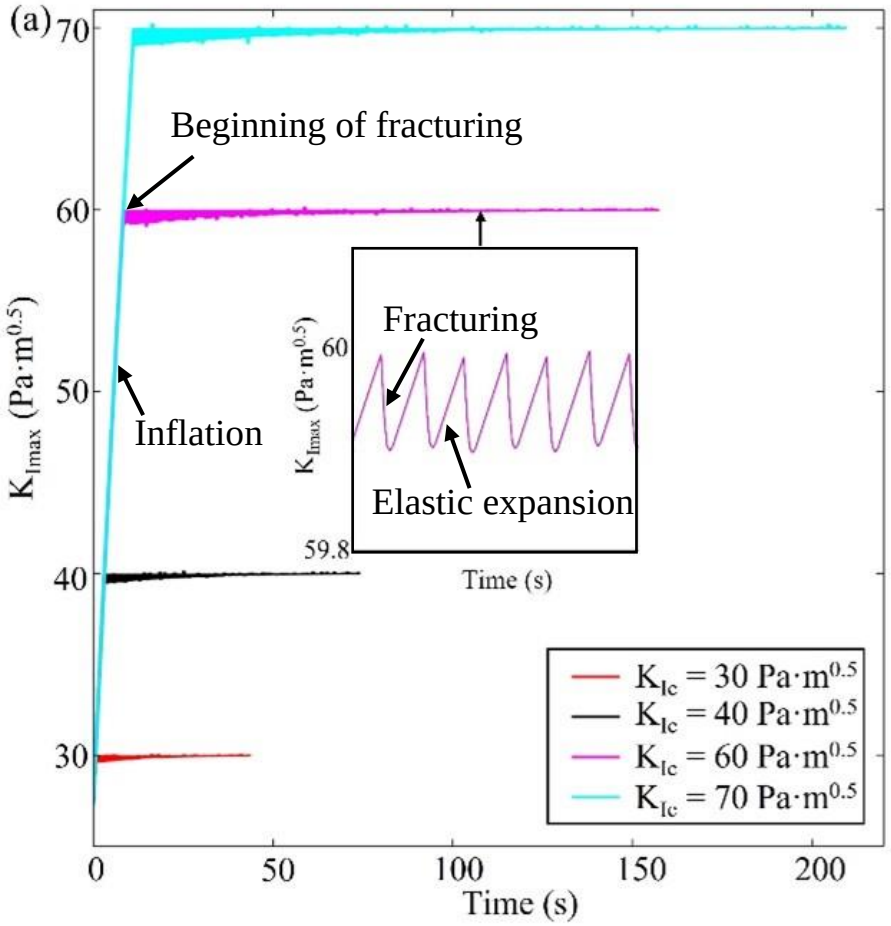

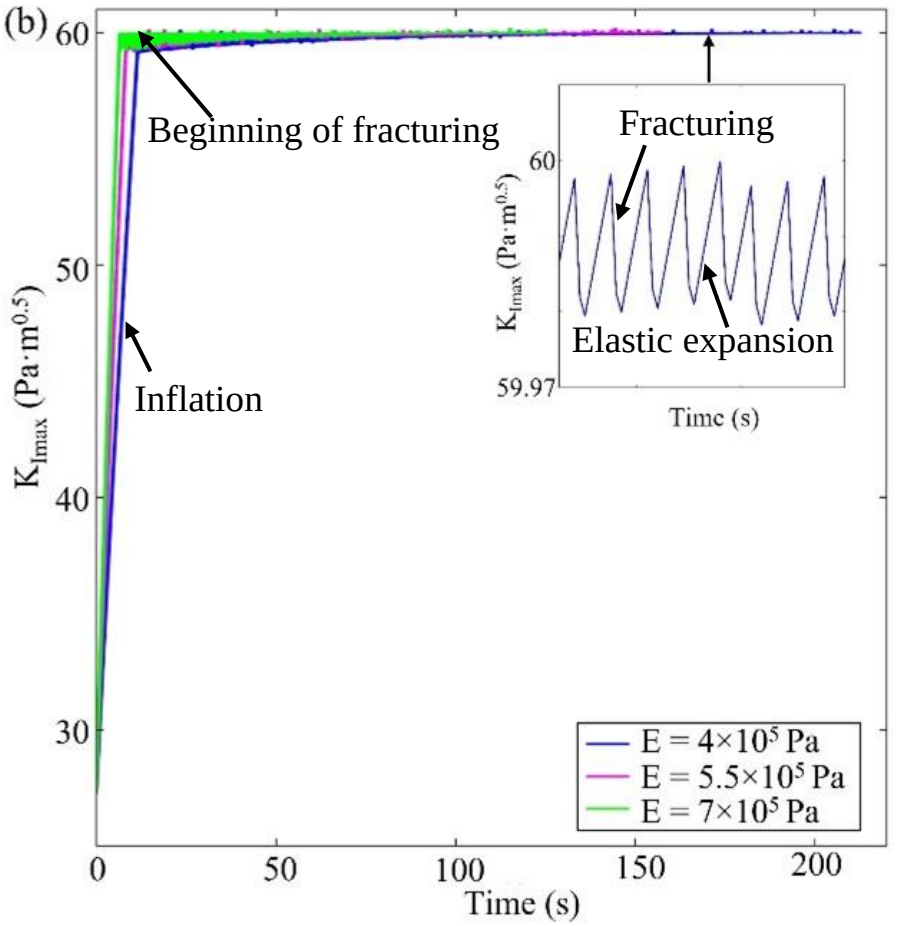

The saw-tooth pattern

5. Results

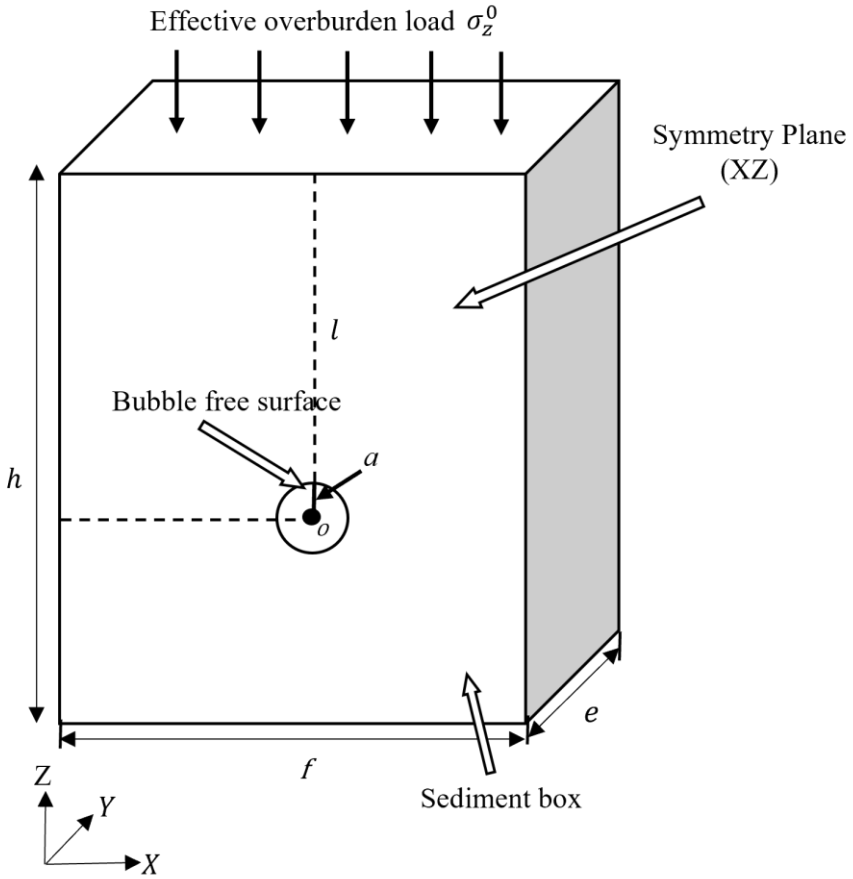

Bubble spatial location Vs Bubble size

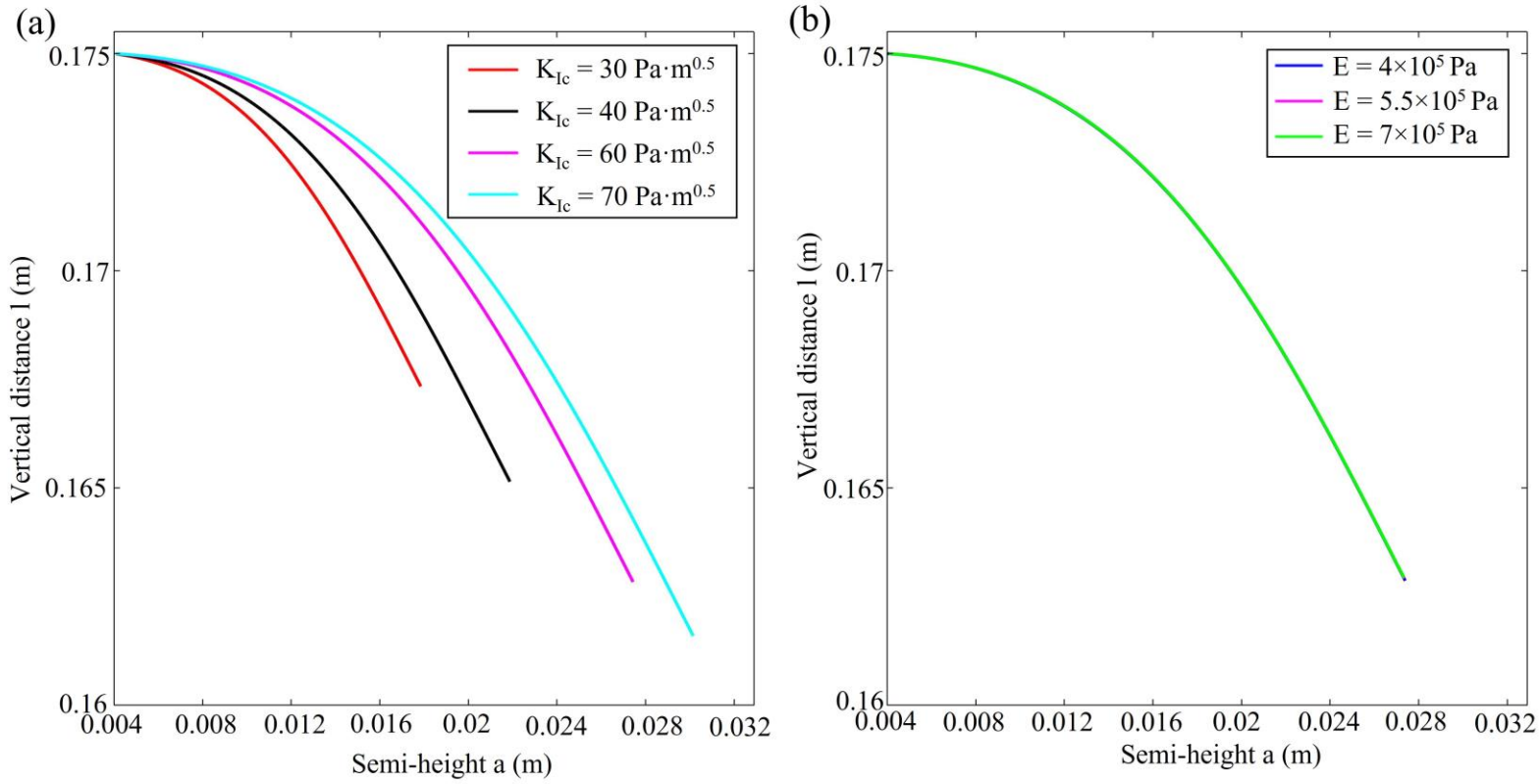

(1) When bubble grows by **fracturing**, its center **moves upwards**, i.e., the distance from the center of the growing bubble to the top of the sediment box, l, decreases, while its vertical size, $2a$, increases.

(2) The distance l is **invariant** with bubble semi-height a, under the different **Young's modules E** (Panel b), but depends on Fracture Toughness K_{Ic} (Panel a).

5. Results

Inner bubble pressure change

(1) The pressure **decreases with time** for all the modelled cases as bubbles grow **preferentially upward**.

(2) Pressure in the stiffer sediment with a larger E decreases faster than in the softer one with a smaller E, due to **the smaller increments** of the pressure drops and thus **shorter subsequent elastic expansion stages**.

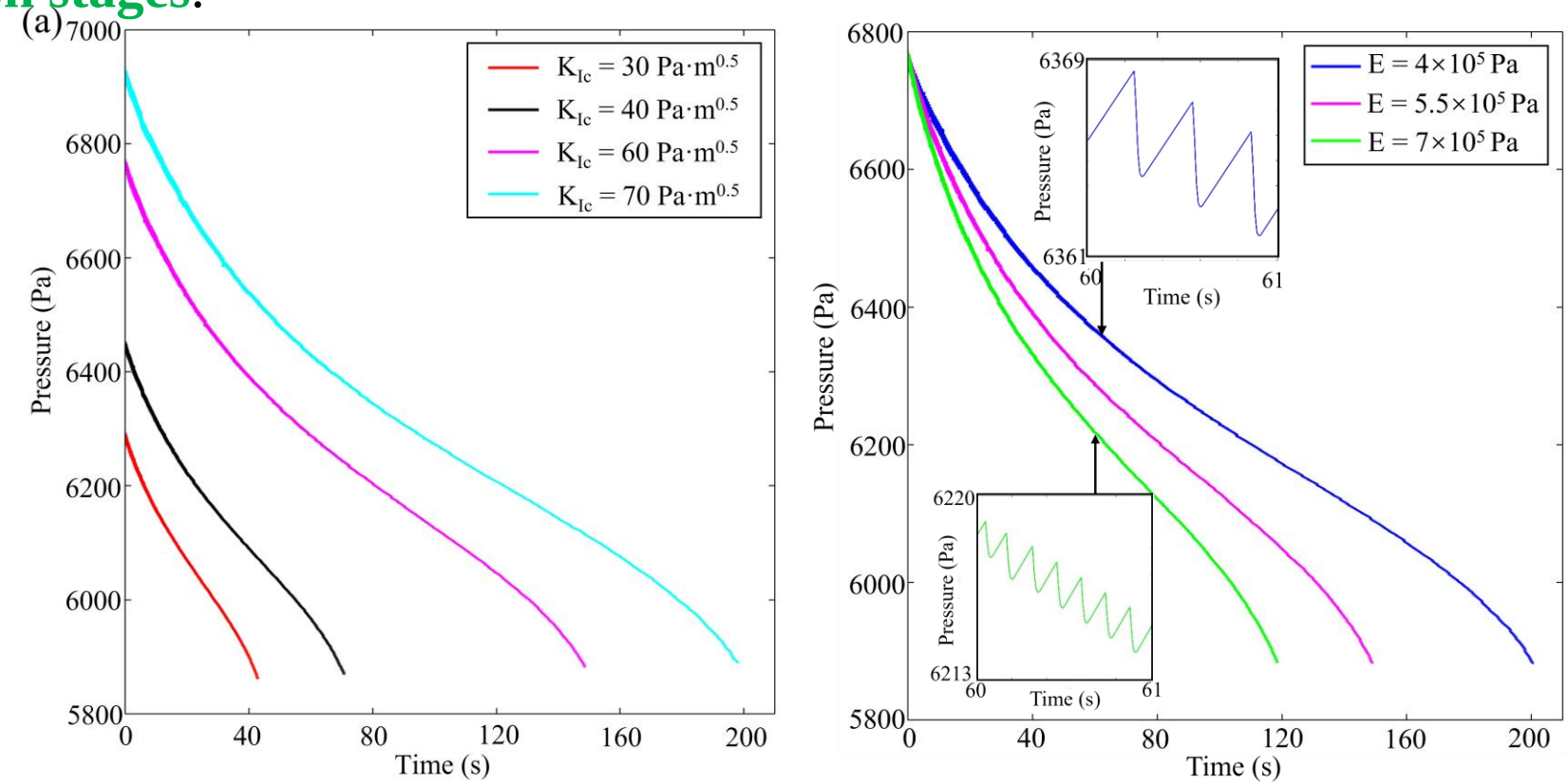

5. Results

Inner bubble pressure vs distance from upper sediment box to bubble center

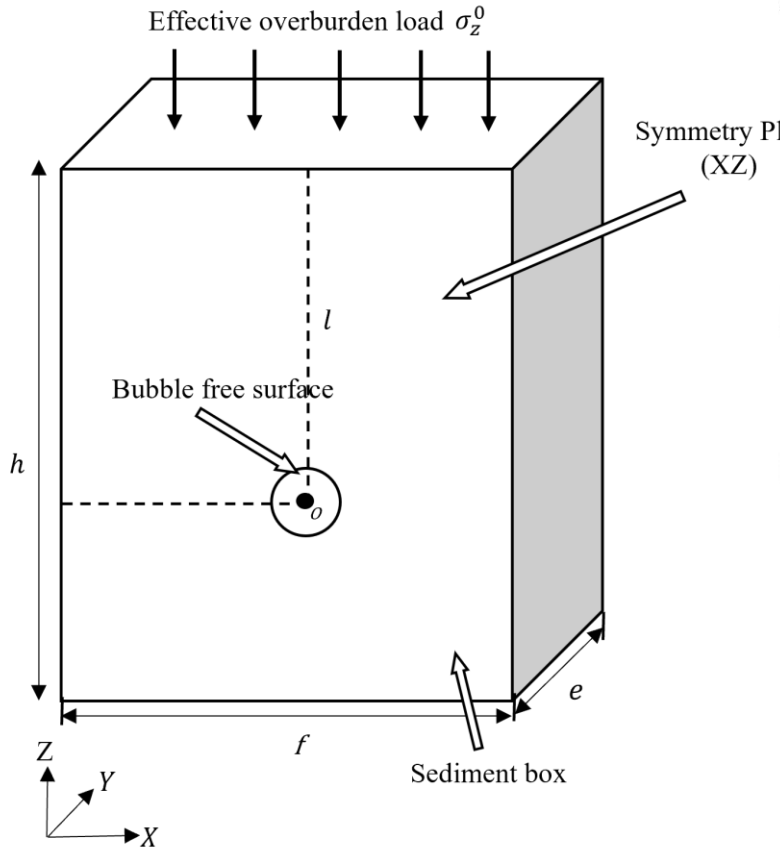

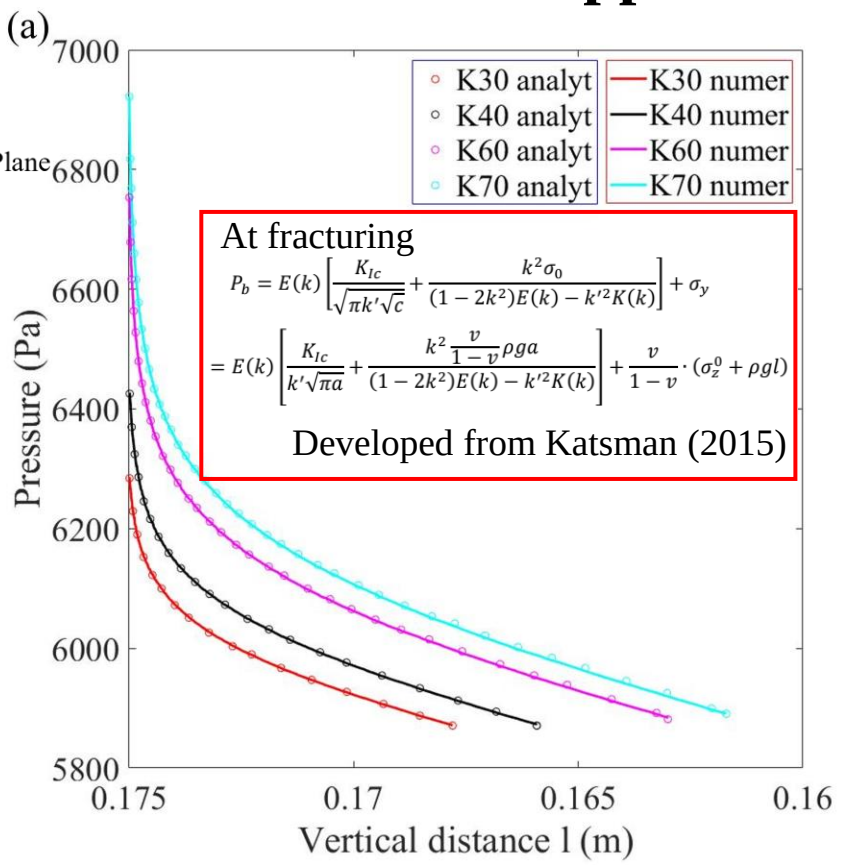

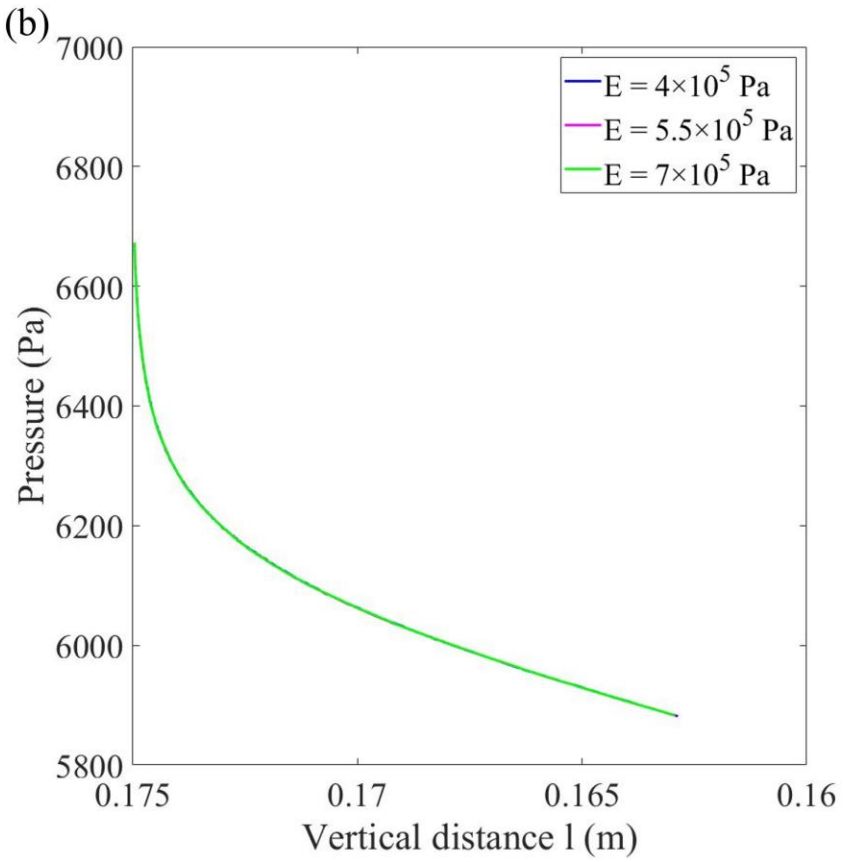

(1) The inner bubble pressure at fracturing associated with each spatial location l of the center of the growing bubble, and with a corresponding growing bubble semi-height a, depends on the K_{Ic} (Panel a) and does not depend on E(Panel b).

(2) The numerical solution shows a good agreement with the analytical solution.

5. Results

Evolution of bubble size and opening under different fracture toughness

(a)

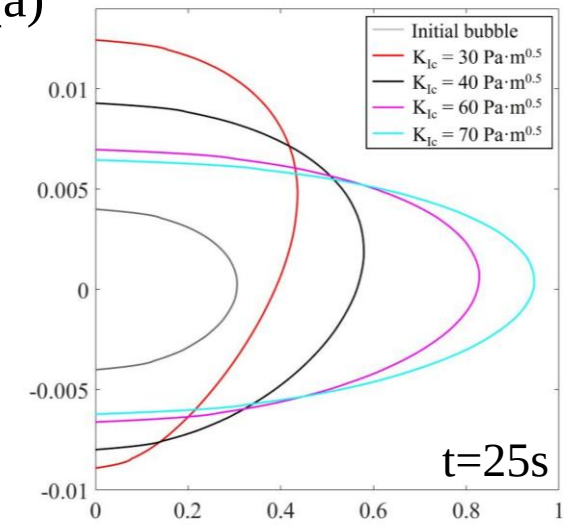

(b)

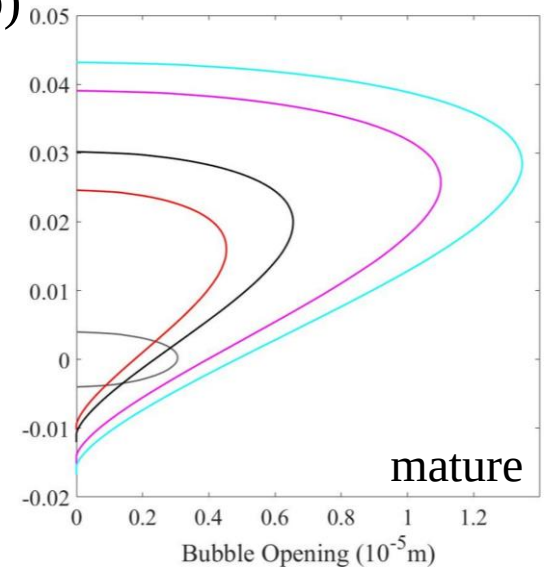

Cross section

(1) At some intermediate moments, e.g., t = 25 s, premature bubbles in sediments with higher Fracture Toughness K_{Ic} (Panel a) are smaller. However, the corresponding mature bubbles' veritical sizes are bigger (Panel b).

(2) Openings of the bubbles demonstrate a bigger maximal opening for bubbles in sediments with higher K_{Ic} (Panels a, b).

(3) The premature bubble openings vary from near ellipsoidal ones in sediments with higher K_{Ic} to nearly inverted tear drop in sediments with lower K_{Ic} (Panel a).

(4) The mature bubble openings for all simulated K_{Ic} cases resemble inverted tear drops (Panel b).

5. Results

Evolution of bubble size and opening under different Young's modulus

(1) At some intermediate moments, e.g., t = 25 s, the bubbles in the stiffer sediments are larger (Panel a), due to their faster growth rates related to higher solute supply rates.

(2) The bubble in the stiffer sediments has a smaller opening at some intermediate moments, e.g., t = 25 s due to smaller pressure at that moment. (Panel a).

(3) The terminal vertical sizes of mature bubbles with different *E* are the same (Panel b), as expected from the analytical predictions (Katsman, 2015).

(4) Those bubbles reveal inverted tear-drop shapes with bigger opening in the sediment with lower *E* (Panel b).

(a)

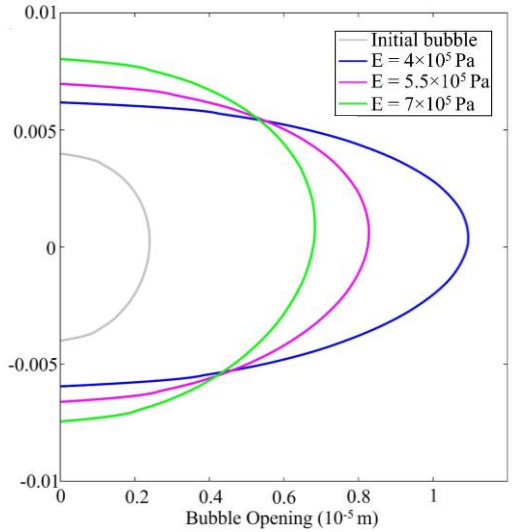

(b)

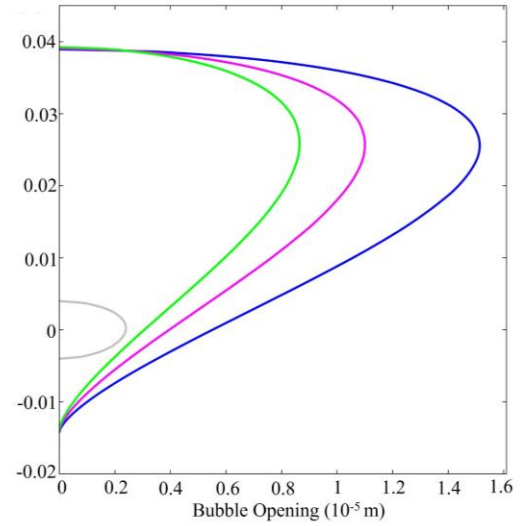

Cross section

5. Results

Total diffusive flux via bubble surface

(1) Total diffusive flux of bubble in sediments with lower K_{Ic} (Panel a) and higher E (Panel b) grows faster with shorter growth time caused by smaller pressure that produces lower local concentrations at its surface, together with a larger bubble temporal size.

(2) The total flux attains larger terminal values for the mature bubbles reaching a higher terminal size in sediments with higher K_{Ic} (Panel a). Almost the same terminal total flux under different E (Panel b) because of the same bubble vertical sizes.

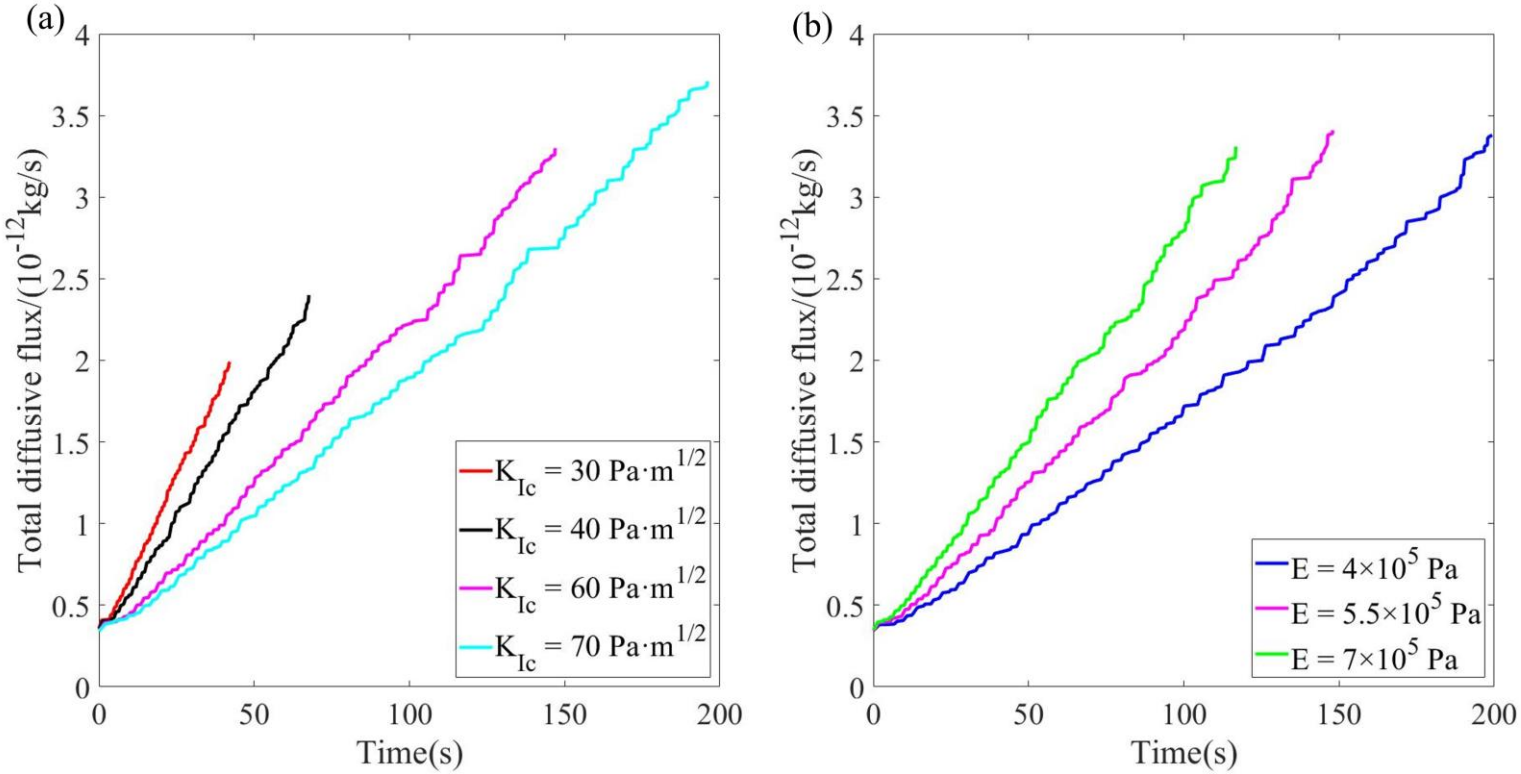

5. Results

Evolution of the total bubble growth time with scaled K_{Ic} and E

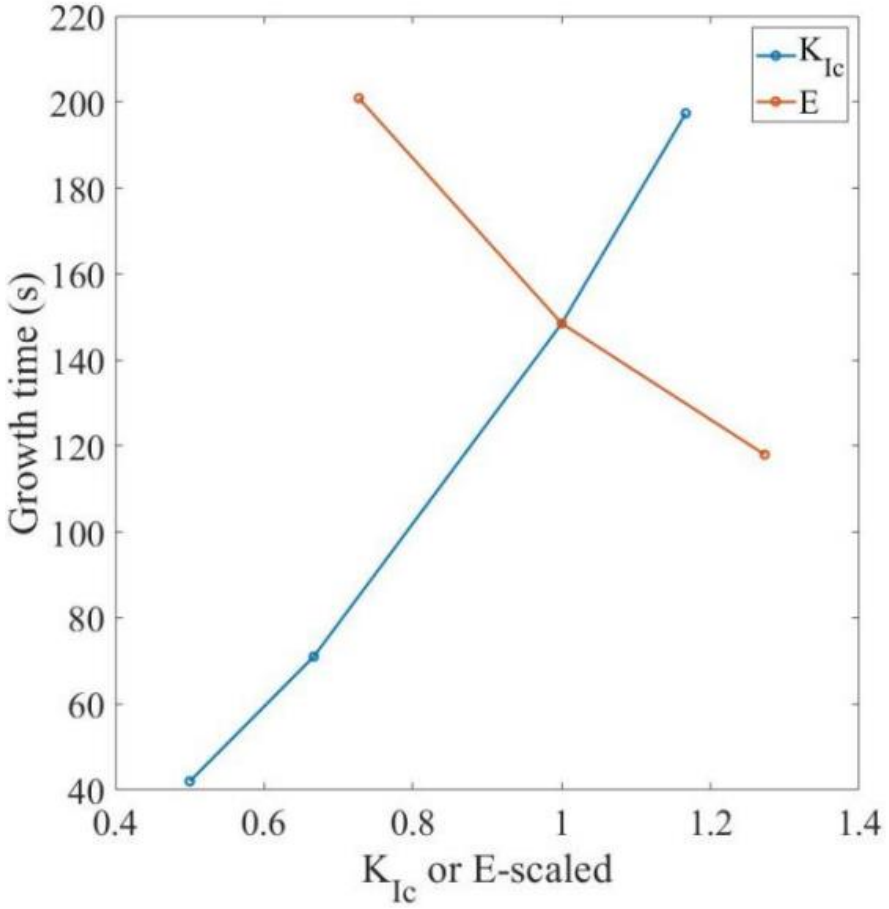

Scaled with their basic values

$K_{Ic} = 60\ Pa \cdot m^{0.5}$**

$E = 5.5 \times 10^5$ Pa**

The evolution of the total bubble growth times till their mature configurations demonstrates that bubble growth time increases with K_{Ic} and decreases with E.

6. Discussion

(1) The prediction of bubble size and opening as a function of K_{Ic} and E

From the developed analytical solutions

Bubble semi-height $a \sim K_{Ic}^{2/3}$

Bubble semi-opening (Maximum opening) $b \sim K_{Ic}^{1/3}\Omega$ $\Omega = \frac{K_{Ic}}{E}$ Constant with depth

Inverse Aspect Ratio $IAR = \frac{b}{a} \sim K_{Ic}^{-1/3}\Omega$

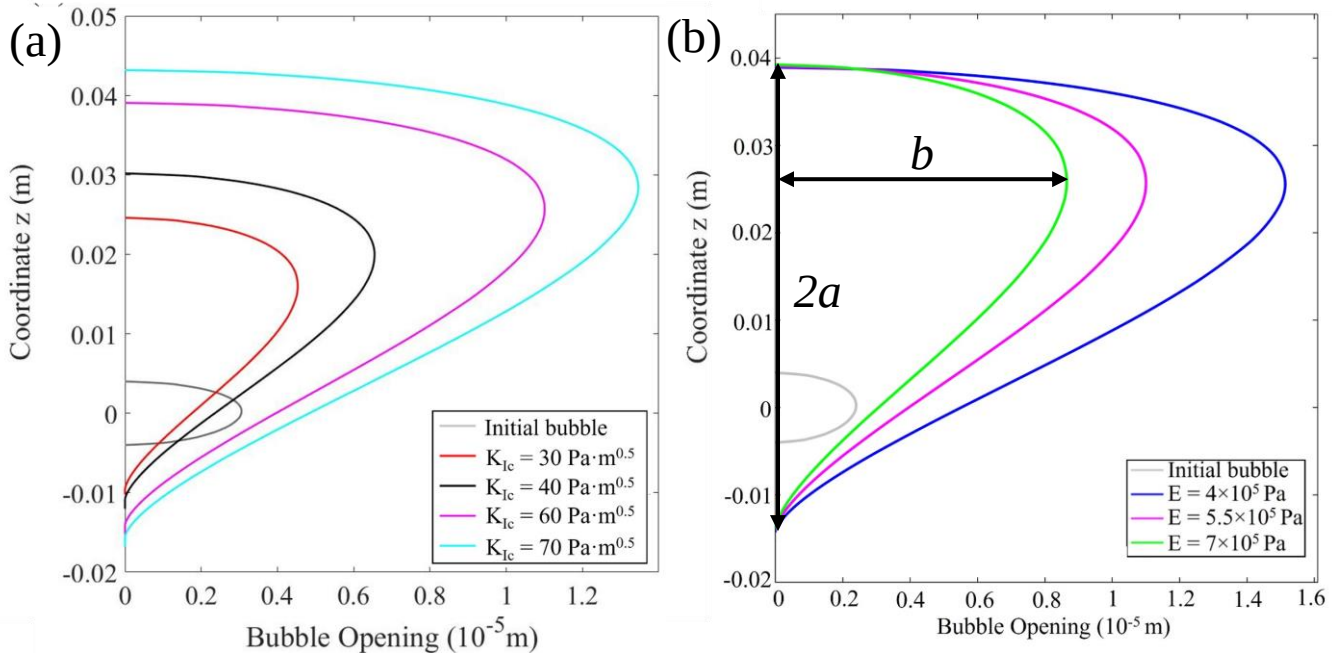

The analytical and numerical analysis well explain a growth of flat long elliptic bubbles in deep sediments and small more spherical ones in the shallow sediments.

The long flat bubbles in the deeper sediments have a bigger sensitivity to solute supply.

6. Discussion

(2) “no-growth” condition

- Insufficient solute supply that sometimes manifested in a potential halt of bubble growth may depend on the ambient solute concentration and also on the bubble internal pressure
- Fluxes and bubble growth rates are almost identical to coupled Ω rather than K_{Ic} and E as suggested by other studies (Algar and Boudreau, 2010)
- It just requires the same pressure and supersaturation to avoid the no-growth stage if Ω is not changed with depth.

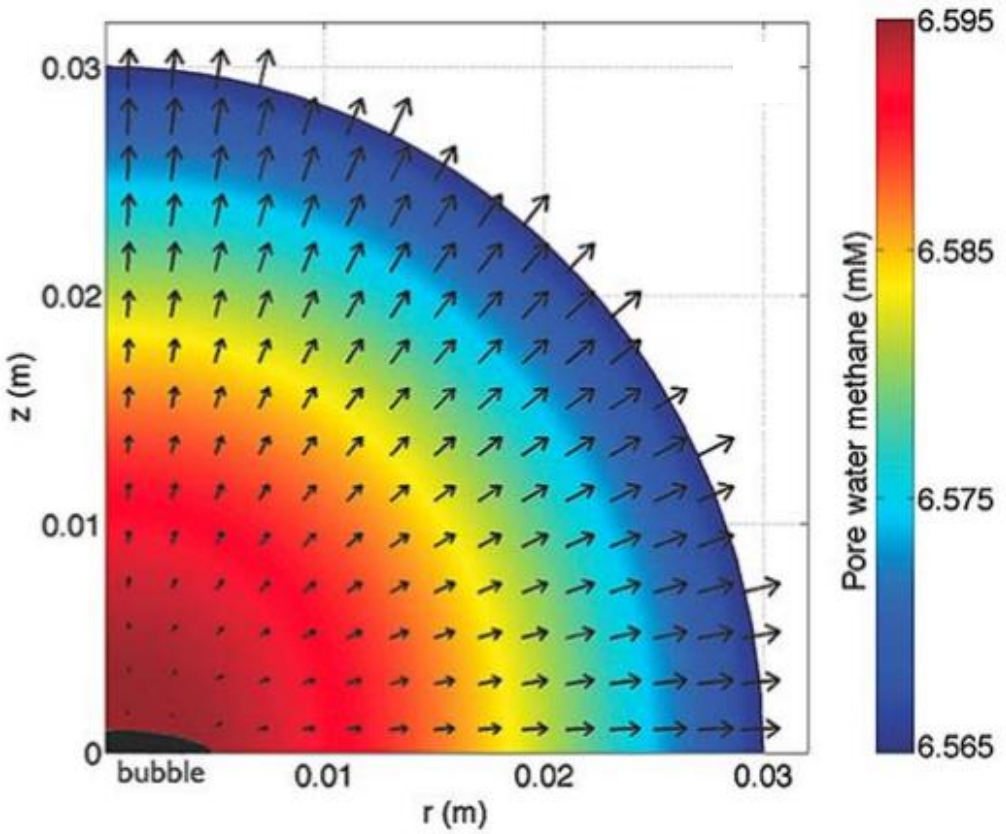

“No-growth” condition as no solute taken by the bubble

One quarter of a slice through the sediment

Algar and Boudreau (2010)

6. Discussion

(3) Implications for competitive bubble growth

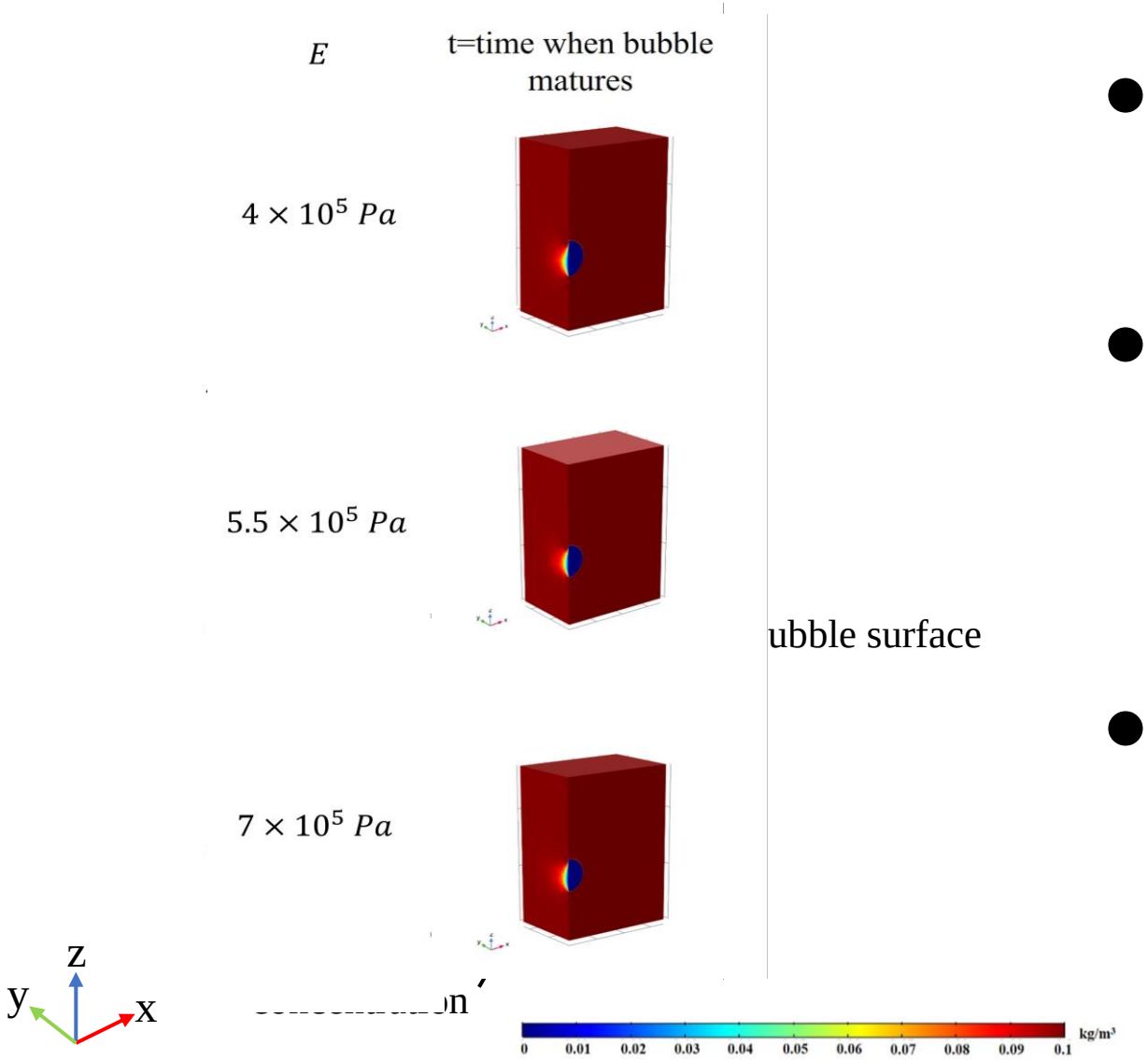

- The depleted concentrations may affect a growth of the adjacent bubbles
- The depleted concentrations area for bubble is larger for bubble in sediments with larger K_{Ic} that affects more competitive bubbles growth
- The depleted concentrations area is almost the same for the sediments with different E due to the same terminal bubble vertical sizes

7. Conclusions

(1) The total bubble growth time and rate increase with sediment Fracture Toughness and decreases with Young's modulus predefined by bigger cumulative CH_4 fluxes via their surfaces. The opposite trends in the Fracture Toughness and Young's modulus effects on the bubble solute fluxes and growth times, and their proportionality specified by LEFM, manage the bubble growth rates. Those are invariant with sediment depth if the ratio K_{Ic}/E is preserved.

(2) Fracture Toughness and Young's modulus are responsible for separate - spatial and temporal - but complementary bubble growth characteristics.

(3) Inner pressure of the growing bubble at fracturing, concentration at its surface, bubble size, shape and spatial location, are defined by sediment Fracture Toughness and do not depend on the Young's modulus.

7. Conclusions

(4) Alternatively, a temporal evolution of the bubble inner pressure at its expansion between the fracturing events depends on the Young's modulus. Smaller increment of bubble inner pressure drop and shorter solute adsorption stage are characteristic for sediments with a bigger Young's modulus.

(5) The analytical model indicates a contribution of the Fracture Toughness to the bubble opening and its surface-to-volume ratio, additional to that specified by the predefined K_{Ic}/E ratio, thus controlling a development of longer flatter bubbles in the deeper sediments.

(6) It is demonstrated for the first time that the mechanical properties of muddy sediments make a significant contribution to the bubble solute fluxes and the bubble growth.

8. Acknowledgements

The financial support of the MSc Fellowships from the University of Haifa

Supervisor, Dr. Regina Katsman

Laboratory mate, Dr. Abhishek Painuly

All the faculty, staff and students in the Department of Marine Geosciences

Parents


Thanks!
Q & A